ENGINEERING APPLICATIONS OF NONHOMOGENEOUS MARKOV CHAINS IN MACHINE LEARNING

Neven Hadžić* – Hrvoje Kozmar – Nikola Vladimir – Marija Koričan – Viktor Ložar

Faculty of Mechanical Engineering and Naval Architecture, University of Zagreb,
Ivana Lučića 5, 10000 Zagreb, Croatia

ARTICLE INFO

***Article history*:**
Received: 12. 2. 2026.
Received in revised form: 16. 7. 2026.
Accepted: 22. 7. 2026.

Keywords:
Machine Learning
Nonhomogeneous Markov chains
Ship and wind speed forecasting
Stochastic process
Transition matrix
Modal superposition method

DOI: 10.30765/er.3217

Abstract:

Machine Learning (ML) methods have been increasingly applied in engineering systems for predictive analytics and decision support. However, their implementation in real-time applications is often limited by computational complexity, memory requirements, and limited interpretability. This study proposes a novel probabilistic ML framework based on nonhomogeneous Markov chains, in which the system state space and transition probability matrix are continuously adapted as new observations become available. The proposed Markov Chain Machine Learning (MCML) methodology was developed by defining adaptive state transitions and evaluating the corresponding limiting probability distributions using both an analytical solution and a modal superposition method (MSM) to reduce computational requirements. The framework was implemented and validated using two physically different cases: purse seiner operational dynamics and high-altitude wind velocity prediction. The obtained results demonstrated excellent consistency between the analytical and MSM approaches, with the mean absolute errors of 0.00424 km/h for the sailing speed and 0.0001 m/s for the wind velocity predictions. The proposed methodology significantly reduces computational complexity while preserving prediction accuracy and probabilistic interpretability, thus providing an efficient framework for real-time engineering applications such as intelligent monitoring, predictive maintenance, and digital twins.

List of abbreviations
AI – Artificial Intelligence
AS – Analytical Solution
CPU – Central Processing Unit
EU – European Union
ML – Machine Learning
MCML – Markov Chains for Machine Learning
MSM – Modal Superposition Method
PH – Prognostic Horizon
LP – Learning Period

* Corresponding author
E-mail address: neven.hadzic@unizg.fsb.hr

1 Introduction

1.1 Overview

Artificial Intelligence (AI) refers to the ability of computer systems to perform tasks that typically require human intelligence, including learning, reasoning, pattern recognition, decision-making, and communication. Over the last decade, AI has become one of the key technologies driving digital transformation in engineering, manufacturing, healthcare, transportation, energy systems, and many other domains [1]. Its rapid adoption has motivated the development of regulatory frameworks, such as the European Union AI Act, aimed at promoting trustworthy, transparent, and human-centric AI while supporting innovation and industrial competitiveness [2], [3]. At the same time, the increasing data availability, advances in computational resources, and continuous algorithm improvements have enhanced AI applications in many disciplines [4]. Despite these advances, AI systems continue to face challenges related to data quality, robustness, scalability, model transparency, and reliable operation in dynamically changing conditions. These issues are particularly evident in Machine Learning (ML), which constitutes the analytical core of most AI systems.

Machine Learning encompasses a broad range of methods that learn patterns from structured and unstructured data to support prediction, classification, optimization, and decision-making. Depending on the learning paradigm, ML algorithms are commonly categorized as supervised, unsupervised, semi-supervised, or reinforcement learning [5]. Their application has expanded to predictive maintenance, smart manufacturing, renewable energy systems, intelligent transportation, healthcare, structural monitoring, computer vision, international shipping, and many other engineering domains [6]–[19]. Nevertheless, developing ML models that simultaneously achieve high predictive accuracy, robustness, adaptability, and computational efficiency in various operating conditions remains a significant challenge.

Recent advances in AI have increasingly focused on developing adaptive and interpretable ML models capable of supporting reliable decision-making [20, 21]. Although deep learning, transformer-based architectures, and foundation models have demonstrated remarkable performance in computer vision, natural language processing, and predictive analytics, their deployment is frequently constrained by high computational demands, extensive training data requirements, considerable energy consumption, and limited model interpretability [22]. Consequently, attention has been devoted to lightweight probabilistic learning methods that combine computational efficiency, explicit uncertainty representation, and transparent decision-making. Such capabilities are particularly important in Industry 4.0, the Industrial Internet of Things (IIoT), digital twins, predictive maintenance, intelligent monitoring, and autonomous control systems, where models are required to continuously adapt to evolving operating conditions while efficiently processing streaming data [23]. Online learning, sequential probabilistic inference, and adaptive state-space modeling have emerged as important research directions for next-generation engineering AI systems [24]. However, many state-of-the-art ML approaches remain based on computationally challenging neural architectures whose complexity limits their deployment in resource-constrained systems [25].

In contrast, probabilistic models based on stochastic processes offer several promising properties, including mathematical interpretability, computational efficiency, explicit uncertainty representation, and suitability for sequential prediction. Markov chain models are particularly well suited for representing stochastic-state transitions while naturally supporting recursive model updating. Despite that fact, the simultaneous adaptation of both the state-space representation and transition probabilities in nonhomogeneous Markov chains remains relatively limited, particularly in the context of adaptive predictive analytics for dynamic engineering applications. Therefore, the present study proposes a novel Machine Learning framework based on nonhomogeneous Markov chains featuring adaptive state-space approach and dynamically updated transition probabilities. Furthermore, building upon the methodology introduced in [26] and [27], the proposed framework incorporates the modal superposition method to substantially reduce computational complexity, thereby enabling efficient implementation in engineering decision-support applications.

1.2 Literature review

The rapid development of AI has enabled extensive work in various domains, including ML, intelligent planning, robotics, natural language processing, computer vision, speech recognition, and expert systems. Recent review studies have systematically summarized these developments while identifying common challenges related to model interpretability, computational scalability, online adaptation, and reliable operation in dynamic environments [4]. Similar conclusions have been reported for ML, where increasing industrial deployment has proven the need for algorithms capable of processing continuous stream of data while maintaining predictive performance in various operating conditions [6]. The efforts have increasingly focused on online learning, continual learning, probabilistic inference, and adaptive predictive modeling for engineering systems requiring sequential data processing and real-time decision support [28]–[30]. Machine Learning models currently employed in engineering applications include statistical learning, graph-based methods, Bayesian inference, Monte Carlo simulations, fuzzy systems, neural networks, reinforcement learning, and probabilistic state-space models, including Markov decision processes and Markov chains [31]–[33]. Probabilistic sequential models have attracted attention because they naturally represent uncertainty while enabling recursive prediction and adaptive modeling [34]. Markov-based approaches represent an important direction for engineering systems characterized by sequential observations and time-dependent state transitions.

Markov chains were introduced into AI using Hidden Markov Models and probabilistic frameworks for speech recognition, handwriting recognition, activity recognition, bioinformatics, Internet modeling, and environmental monitoring [35]. Their capability to represent stochastic-state transitions has subsequently led to numerous applications in robotics, autonomous systems, natural language processing, transportation, and intelligent monitoring [36]–[40]. More recently, Markov-based models have been employed in predictive maintenance, digital twins, autonomous control, and industrial decision-support systems, where probabilistic prediction has become important [41, 42]. In parallel, other AI techniques, particularly artificial neural networks, have been used in maritime engineering, including the prediction of the ship main-engine power demand, fuel consumption, and pollutant emissions [15], demonstrating the growing role of data-driven methods in optimal ship operation.

Despite their successful application, several limitations have been identified. Large transition spaces often create high computational and memory requirements together with increased prediction latency [36]–[40]. These challenges become even more pronounced when the state spaces evolve over time or when models must continuously incorporate newly acquired observations. Recent efforts have increasingly focused on the reduced-order modeling, approximation techniques, online parameter estimation, and efficient probabilistic learning algorithms capable of maintaining predictive accuracy while reducing computational requirements [43]–[45].

The application of Markov chains has evolved in the ML systems. Studies have considered wind-power forecasting, electrical transport modeling, rainfall prediction, urban dynamics, poroelasticity, database evolution, supply-chain optimization, and disease-risk assessment [46]–[53]. In many cases, Markov chains are combined with complementary techniques such as Monte Carlo simulation, neural networks, cellular automata, Bayesian inference, and Extreme Learning Machines to improve predictive performance [54]. Nevertheless, most existing Markov-based frameworks rely on homogeneous transition probabilities and fixed-state representations, limiting their ability to accurately describe non-stationary engineering processes characterized by evolving system dynamics [55]. The increasing application of AI in contemporary engineering systems has introduced additional requirements for ML algorithms, mainly related to real-time implementation [56, 57]. Although deep learning approaches have demonstrated outstanding predictive capabilities, their computational complexity and limited interpretability often restrict their applicability in resource-constrained engineering environments. These limitations have renewed interest in lightweight probabilistic models that combine computational efficiency, explicit uncertainty representation, and transparent sequential prediction, making them suitable for engineering decision-support applications [34].

Based on the literature survey, three important research gaps can be identified. First, existing Markov-based ML frameworks predominantly rely on homogeneous transition probabilities, limiting their ability to assess non-stationary system dynamics. Second, the state-space representation is generally fixed during model development, preventing adaptive refinement as new data become available. Third, although computational complexity has been recognized as a major limitation of large-scale Markov models, some studies simultaneously address model adaptability and computational efficiency required for engineering applications. Therefore, the present study proposes a novel Machine Learning framework based on nonhomogeneous Markov chains in which both transition probabilities and the state-space representation are continuously updated during the learning process. This framework is intended to provide adaptive predictive analytics for engineering systems operating in dynamic conditions.

2 Modeling

2.1 Basic information

The modeling approach considered two approaches, i.e., the analytical solution and the approximative method employing the modal superposition method to reduce computational requirements. A decrease in the number of modes considered was carefully considered in the second case to investigate the possibility of additional CPU reductions. The analytical solution was employed to validate the approximative approach and to identify the best possible option for the application of nonhomogeneous Markov chains on AI and ML. The proposed framework assumes that the studied processes can be approximated by a first-order nonhomogeneous Markov chain in the selected sampling interval. While the underlying physical system may exhibit longer temporal dependencies, the current state is assumed to contain sufficient information, especially as the adaptive state-space representation and continuously updated transition probabilities further mitigate the effect of slowly varying process dynamics.

2.2 The analytical solution

Consider a stochastic system randomly shifting its states in the system state space of a priori unknown scale, or unknown horizon. Assume that the state of the system is recorded in equally distributed time instants or cycles with the system database, e.g., in the form of a signal, Figure 1. The behavior of such a system can be represented by employing nonhomogeneous Markov chains. The probability of the system to be in the state X in cycle n, $\{\pi\}_n$, is [58]:

$$\{\pi\}_n = \left[P(n)\right]\{\pi\}_{n-1},\ n>1, \tag{1}$$

where $\left[P(n)\right]$ is the transition matrix of a nonhomogeneous Markov chain and $\{\pi\}_{n-1}$ is the probability distribution associated with cycle *n*-1. For *n*=1, the probability distribution $\{\pi\}_0$ corresponds to the initial state of the system. Note that the transition matrix $\left[P(n)\right]$ is a function of the cycle number both in terms of transition probabilities, $p_{ij}(n)$, and in terms of matrix dimension, $d(n)\times d(n)$. The dimension of column vectors $\{\pi\}_n$ and $\{\pi\}_{n-1}$ is accordingly updated concerning the possible identification of new states.

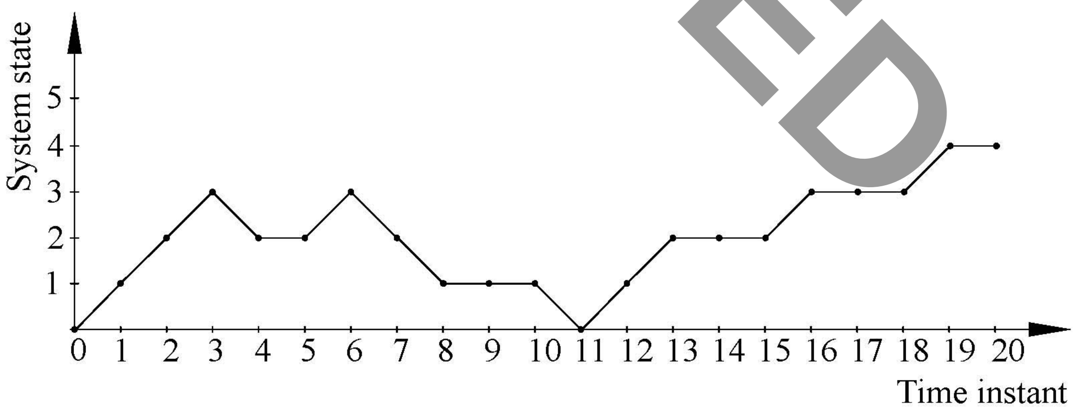

Figure 1. An example of the system database in the form of a random signal

The transition matrix, $\left[P(n)\right]$, is composed of transition probabilities, $p_{ij}(n)$, equal to:

$$p_{ij}(n) = \frac{m_{ij}(n)}{M_i(n)}, \tag{2}$$

where $m_{ij}(n)=\sum_{n>0}1_{\{X_n=j|X_{n-1}=i\}}$ is the total number of visits from the state $X_{n-1}=i$ to the state $X_n=j$, while $M_i(n)=\sum_{n>0}1_{\{X_{n-1}=i\}}$ is the total number of visits to the state $X_{n-1}=i$. The matrix dimension, $d(n)$, is defined as:

$$d(n)=\sum_{n>0}1_{\{X_n\notin\{H\}_n\}}, \tag{3}$$

where $\{H\}_n$ is the system state space horizon associated with the cycle *n* and defined as a set of all states recognized since the initialization of the data acquisition. In that way, the transition matrix, $\left[P(n)\right]$, may be perceived as the system transition inventory which can be employed in each cycle to evaluate the associated long-term probability distribution of the system, $\{\pi\}_{n\to\infty}$, to obtain the predictive analytics in the form of the expected system behavior. Thus, for a sufficiently large *n*, the relationship [58]:

$$\{\pi\}_n=\left[P(n)\right]\{\pi\}_n, \tag{4}$$

is considered appropriate. The system of equations (4) may be solved by direct multiplication of transition matrices as:

$$\{\pi\}_n=\left[P(n)\right]^n\{\pi\}_0, \tag{5}$$

or as an eigenvalue problem [59]:

$$\left(\left[P(n)\right]-\Omega_i\left[I\right]\right)\{\pi\}_i=0, \tag{6}$$

where Ω_i is the unknown eigenvalue, $\left[I\right]$ is the unit matrix, and $\{\pi\}_i$ is an eigenvector associated with i^{th} eigenvalue. Since the transition matrix is also a stochastic one, its first and the largest eigenvalue always takes a unit value, i.e., $\Omega_i=1$. The first eigenvector, $\{\pi\}_1$, associated with Ω_1, represents the unique and limiting probability distribution, usually referred to as the stationary probability distribution, provided the Markov chain satisfies the ergodicity criteria on reducibility and periodicity and the Dobrushin's ergodic coefficient [60].

A homogenous Markov chain is ergodic if it is irreducible and aperiodic. These two conditions may easily be verified by inspecting the structure of the transition matrix. A Markov chain is thus irreducible if all states have a property of mutual communication, i.e., there are no separate classes of system states. A Markov chain is aperiodic if at least one diagonal element is larger than zero. In addition, a nonhomogeneous Markov chain must satisfy the criteria on weak and strong ergodicity. A nonhomogeneous Markov chain is weakly ergodic if the associated Dobrushin's ergodic coefficient δ meets the condition $\lim_{n\to\infty}\delta=0$, where:

$$\delta=\frac{1}{2}\sup_{i,j}\sum_k\left|p_{ik}(n)-p_{jk}(n)\right|. \tag{7}$$

Here, Eq. (7) and the limiting condition may be interpreted as a fading difference between rows of the transition matrix. Finally, each weakly ergodic nonhomogeneous Markov chain is considered strongly ergodic if it satisfies the conditions regarding irreducibility and aperiodicity. The stationary probability distribution of a strongly ergodic Markov chain is a unique limiting probability distribution which can be further employed to integrate nonhomogeneous Markov chains as a continuously updatable model within AI and ML frameworks.

2.3 The modal superposition method

The presented analytical solution, Eq. (5), for a straightforward and thorough approach to predictive analytics is unfortunately characterized by substantial CPU costs and memory storage requirements, so it cannot be directly employed in real-life cases of large and transition-rich systems possibly involving myriads of communicating states. Hence, an approximative method of the modal superposition of modes may be considered as an alternative approach to the problem ensuring a reasonable tradeoff between computing requirements and the reliability of the results. Therefore, consider an eigendecomposition of the transition matrix, $\left[P(n)\right]$, as:

$$\left[P(n)\right]=\left[U(n)\right]\left[\Omega(n)\right]\left[V(n)\right]^{\mathrm{T}}. \tag{8}$$

where $\left[U(n)\right]$ and $\left[V(n)\right]$ are matrices with the right-hand, respectively left-hand side eigenvectors of the transition matrix, $\left[\Omega(n)\right]$, which is a diagonal matrix with eigenvalues $\Omega_1(n)$, $\Omega_2(n)$, …, $\Omega_{d(n)}(n)$, and $d(n)$ as the total number of states, Eq. (3), [60]. An introduction of Eq. (8) into Eq. (1) yields:

$$\{\pi\}_n=\left[U(n)\right]\left[\Omega(n)\right]\left[V(n)\right]^{\mathrm{T}}\{\pi\}_{n-1},\; n>1. \tag{9}$$

which can be more conveniently presented in the modal form as:

$$\{\pi\}_n=\sum_{i=1}^{d(n)}\Omega_i\left\{u(n)\right\}_i\left\langle v(n)\right\rangle_i\{\pi\}_{n-1},\; n>1. \tag{10}$$

Several important remarks regarding Eq. (10) need to be mentioned at this point. First, the problem of ML and predictive analytics can be conveniently reduced to a well-known eigenvalue problem potentially reducing high computational requirements. Second, the transition matrix is usually an asymmetric matrix with real entries. Its eigenvalues and eigenvectors may consequently appear in the real and complex conjugate forms except for the first eigenvalue which is equal to one. However, since $\mathrm{Im}(\Omega_i) << \mathrm{Re}(\Omega_i)$, $\mathrm{Im}\{u\}_i << \mathrm{Re}\{u\}_i$, and $\mathrm{Im}\langle v\rangle_i << \mathrm{Re}\langle v\rangle_i$, $i=2,3,...,d(n)$, the imaginary part may be neglected from the calculation as values of significantly lower order of magnitude [59]. Third, the unknown eigenvalues and eigenvectors can be calculated by employing one of the established procedures, e.g., the Power method and QR method [61]. However, this could easily become inconvenient as it may lead to an increase in computational requirements accompanied by numerical stability and accuracy issues, which is contradictory to the motivation of the present work. Therefore, a limited number of eigenvalues can be considered in Eq. (10) enabling agile and reliable implementation of the nonhomogeneous Markov chains. Fourth, in the case when an observed system shifts in a controlled fashion, similarly to a random walk only between neighboring states, the eigenvalues and associated eigenvectors can be evaluated analytically based on the transition matrix of a priori known structure [59]. However, this is only a special case of more general systems considered in this study.

In addition to the above remarks, it should be emphasized that in the proposed nonhomogeneous framework, the limiting probability distribution is associated with the current transition probability matrix rather than with the entire time-evolving stochastic process. Since the transition probabilities are continuously updated as new observations become available, the corresponding limiting distribution should be interpreted as a locally valid probabilistic prediction that remains applicable only until the next matrix update. Consequently, instead of converging to a single stationary distribution, the proposed methodology creates a sequence of adaptive limiting probability distributions that evolve together with the monitored process. This enables the model to continuously reflect changes in system dynamics while preserving the probabilistic interpretation of the Markov framework.

2.4 Evaluation methodology

Both approaches, the analytical solution (AS) and the modal superposition method (MSM), were formally integrated in the AI and ML framework in the form of an in-house program 'Markov Chains for ML' (MCML) by employing a Fortran programming language [62]. The key ability of the MCML program is the efficient formulation of the transition matrix, $\left[P(n)\right]$, based on the data transmitted by sensors and conditioned to the time elapsed from the start of data acquisition. Upon its formulation, the transition matrix, $\left[P(n=N)\right]$, can be further employed to evaluate the probability distribution, $\{\pi\}_{n=PH}$, associated with the targeted prognostic horizon, *PH*, specified by the user. Such a probability distribution can be evaluated by employing an analytical solution, (AS), Eq. (5), or through a modal superposition method (MSM), Eq. (10). In the former case, the information on the initial state of the system, $\{\pi\}_{n=0}$, needs to be provided, while in the latter case, user must specify the intended number of modes, $d(n)$. A flow chart of the evaluation methodology in the MCML program is presented in Figure 2.

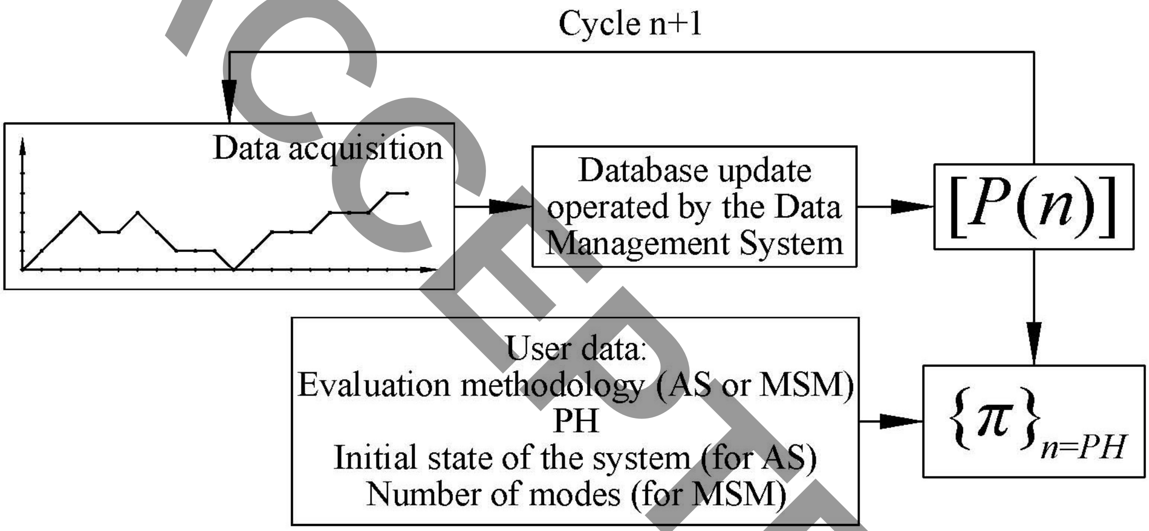

Figure 2. Flow chart of the evaluation methodology included in the MCML program

3 The application of the developed approach

3.1 Basic information

The developed approach was applied in the case of two databases acquired in experimental campaigns. The first one represents a record of the ship performance regarding the sailing speed governed by the operative and environmental conditions at open sea. The second one includes a time history of the high-altitude wind flow velocity in the atmospheric boundary layer. In both cases, the acquired track records contain a significant amount of data which may be understood as a random data collection or a random signal. Hence, both random signals were considered by applying the developed theory to obtain the associated predictive analytics. First, each case was evaluated by employing the direct analytical solution (AS), Eq. (5), as well as the modal superposition method (MSM), Eq. (10), to assess the possibility of the CPU cost reduction conditioned to the reliability of the results. Second, the impact of the learning period (LP) as well as that of the prognostic horizon (PH) on the reliability of estimates was considered. Third, a relationship between the system state space discretization level and the accuracy of the estimates was observed to study the possibility of additional CPU and data storage reductions through aggregation of system states.

3.2 The sailing speed of a purse seiner

A purse seiner is a type of fishing vessel that uses a fishing net to encircle a fish school and catch large quantities of pelagic species or tuna. Its usual operating interval ranges between 15 and 20 hours daily with most of the time dedicated to cruising, silent idling, and fish hauling. This in turn yields a diverse operative profile [63]. However, the complexity of its operative profile together with the harsh environmental conditions hinders further calculations like the expected operative costs, fuel consumption, and environmental emissions. Therefore, it is of interest to model the sailing speed of a purse seiner as a nonhomogeneous Markov Chain in the ML framework to obtain the expectations associated with each sailing speed and to enable further evaluation of the critical operative properties for a dedicated prognostic horizon. For this purpose, a purse seiner was equipped with Mapon fleet management software providing an effective and simple way to remotely track vehicles using a Global Position System [64, 65]. The data considered was acquired in the Adriatic Sea between January 14, 2023, and April 19, 2024. In total, 51733 sailing speed data points were acquired during ship activity with a 10 s sampling cycle. An example of a sailing speed fluctuation in the case of a typical operative profile of the monitored purse seiner is shown in Figure 3. The same data were employed here according to the methodology included in the MCML program.

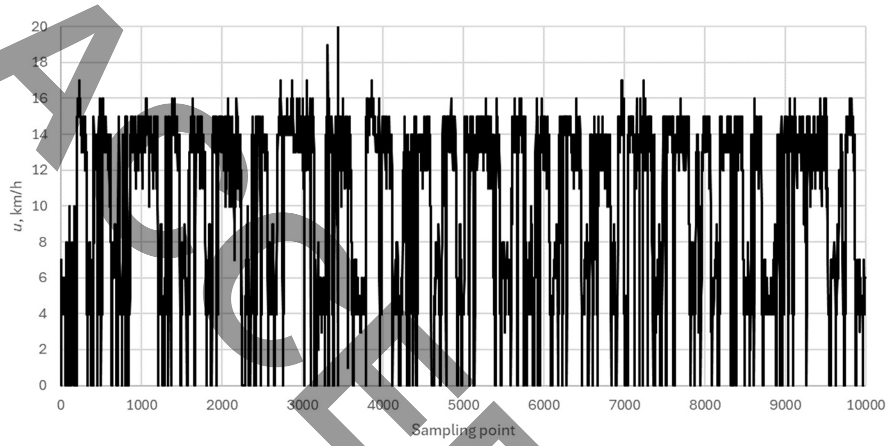

Figure 3. An example of the sailing speed acquired using Mapon software during the first 10000 cycles of a purse seiner

The acquired data was considered in several cases including three learning periods (January to June 2023, January to December 2023, and January 2023 to April 2024) and two prognostic horizons (100 and 1000 cycles). In each case, a probability distribution, $\{\pi\}$, was calculated by employing the AS and MSM procedure, Eqs. (1) and (10), respectively. It is important to point out that only the first eigenvalue, $\Omega_1 = 1$, and the associated eigenvectors, $\{u\}_1$ and $\{v\}_1$, were considered in the case of the MSM procedure. This follows directly from the spectral properties of the ergodic Markov chains. Since the magnitudes of all remaining eigenvalues are smaller than one, their contributions decay exponentially with increasing prognostic horizon and they represent only transient dynamics. A detailed analysis of the transient modal response and the influence of higher-order modes is available in [59]. The results obtained are presented in Table 1. In total, 21 different sailing speeds between 0 km/h and 20 km/h were identified in the case of each learning period. It is to be noted that the probability distributions associated with AS and MSM procedures slightly differ when PH equals 100 cycles, indicating the possible transient effects of the Markov chain. However, in the case when PH equals 1000 cycles, they yield the same results regardless of the learning period.

Each probability distribution is further employed to calculate the expected sailing speed, u_E, as:

$$u_E = \sum_{i=1}^{d} u_i \pi_i \ . \tag{11}$$

where u_i, i=1, 2, …, d, is the identified sailing speed, π_i is the associated element of the probability distribution vector, and d is the total number of identified states. The obtained expected sailing speeds are compared with the statistically averaged values, demonstrating very good agreement since the same learning periods are considered as statistical samples. In addition, the predicted standard deviations closely match the statistical ones, confirming that the proposed model can be successfully used to assess both the central tendency and the dispersion of the sailing-speed distributions. Finally, both the expected and statistically averaged sailing speeds slightly increase with the learning period, indicating that the effect of the observation period together with possible changes in the operating profile of the vessel.

Table 1. Probability distributions and the expected sailing speed determined for three learning periods (LP) and two prognostic horizons (PH)

	LP – January to June 2023				LP – January to December 2023				LP – January 2023 to April 2024			
	PH=100 cycles (1000 s)		PH=1000 cycles (10000 s)		PH=100 cycles (1000 s)		PH=1000 cycles (10000 s)		PH=100 cycles (1000 s)		PH=1000 cycles (10000 s)	
Sailing speed, km/h	AS	MSM	AS	MSM	AS	MSM	AS	MSM	AS	MSM	AS	MSM
0	0.089	0.078	0.078	0.078	0.084	0.080	0.080	0.080	0.075	0.072	0.072	0.072
1	0.001	0.001	0.001	0.001	0.001	0.001	0.001	0.001	0.001	0.001	0.001	0.001
2	0.000	0.000	0.000	0.000	0.001	0.001	0.001	0.001	0.001	0.001	0.001	0.001
3	0.003	0.002	0.002	0.002	0.002	0.002	0.002	0.002	0.001	0.001	0.001	0.001
4	0.089	0.079	0.079	0.079	0.043	0.041	0.041	0.041	0.035	0.033	0.033	0.033
5	0.087	0.077	0.077	0.077	0.043	0.040	0.040	0.040	0.034	0.033	0.033	0.033
6	0.061	0.055	0.055	0.055	0.030	0.029	0.029	0.029	0.024	0.023	0.023	0.023
7	0.044	0.040	0.040	0.040	0.023	0.022	0.022	0.022	0.018	0.018	0.018	0.018
8	0.036	0.034	0.034	0.034	0.019	0.019	0.019	0.019	0.016	0.016	0.016	0.016
9	0.017	0.017	0.017	0.017	0.028	0.028	0.028	0.028	0.028	0.028	0.028	0.028
10	0.013	0.013	0.013	0.013	0.027	0.027	0.027	0.027	0.030	0.030	0.030	0.030
11	0.018	0.019	0.019	0.019	0.026	0.026	0.026	0.026	0.030	0.030	0.030	0.030
12	0.047	0.050	0.050	0.050	0.060	0.061	0.061	0.061	0.069	0.069	0.069	0.069
13	0.132	0.142	0.142	0.142	0.170	0.173	0.173	0.173	0.194	0.196	0.196	0.196
14	0.247	0.268	0.268	0.268	0.312	0.317	0.318	0.317	0.318	0.323	0.323	0.323
15	0.103	0.112	0.112	0.112	0.115	0.117	0.117	0.117	0.107	0.109	0.109	0.109
16	0.012	0.013	0.013	0.013	0.013	0.014	0.014	0.014	0.013	0.013	0.013	0.013
17	0.001	0.001	0.001	0.001	0.002	0.002	0.002	0.002	0.002	0.002	0.002	0.002
18	0.000	0.000	0.000	0.000	0.000	0.000	0.000	0.000	0.000	0.000	0.000	0.000
19	0.000	0.000	0.000	0.000	0.000	0.000	0.000	0.000	0.000	0.000	0.000	0.000
20	0.000	0.000	0.000	0.000	0.000	0.000	0.000	0.000	0.000	0.000	0.000	0.000
Expected sailing speed, u_E, and (standard deviation), km/h	9.737 (4.937)	10.189 (4.816)	10.189 (4.816)	10.189 (4.816)	10.964 (4.622)	11.095 (4.552)	11.109 (4.550)	11.095 (4.552)	11.254 (4.387)	11.361 (4.325)	11.361 (4.325)	11.361 (4.325)
Statistically average sailing speed, $\bar{u}$, and (standard deviation), km/h	10.176 (4.819)				11.101 (4.605)				11.370 (4.335)			
Absolute difference, $u_E - \bar{u}$, km/h	0.439	-0.013	-0.013	-0.013	0.137	0.006	-0.008	0.006	0.116	0.009	0.009	0.009

In addition to comparing the predicted limiting probability distributions with the statistical characteristics of the corresponding learning periods, the shortest learning period (January–June 2023) was further employed to evaluate the predictive capability of the proposed framework during a subsequent prognostic horizon of 1000 cycles. For this purpose, the transition matrix [P], Eq. (2), estimated from the learning period was combined with a random number generator, while a sailing speed of 0 km/h corresponding to the last cycle of the learning period was selected as the initial state. The resulting stochastic simulation represents an out-of-sample prediction when the transition probabilities identified from the learning period are used to create sailing-speed trajectories beyond the training interval. Owing to the stochastic nature of the proposed model, infinitely many trajectories may be generated. A representative trajectory is shown in Figure 4 together with the corresponding sailing-speed measurements acquired by the MAPON system during the same prediction interval. Although an individual simulated trajectory is not expected to reproduce the measured sequence exactly, the comparison demonstrates that the proposed framework successfully models the overall stochastic behavior and the statistical characteristics of the subsequently observed process.

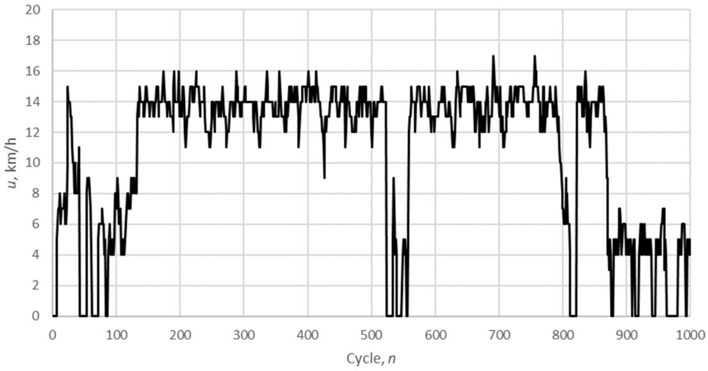

a)

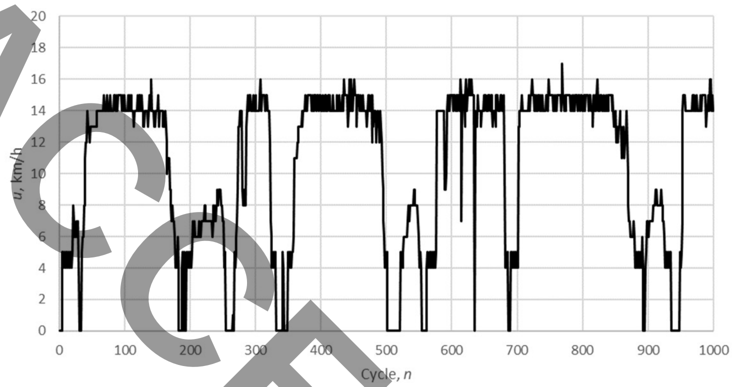

b)

Figure 4. a) The projected trajectory of the sailing speed fluctuation in comparison with b) the data acquired during the same time frame, LP – January to June 2023, PH – 1000 cycles

3.3 The high-altitude wind velocity

The high-altitude wind velocity is physically a completely different phenomenon. However, from the modeling point of view, it can be formulated using the same approach of the nonhomogeneous Markov chain. The predictive analytics of wind flow velocity and other weather conditions may be obtained and further used to evaluate e.g., the wind conditions of wind turbines and the associated energy-harnessing potential. The same approach can also be used to improve the wind-turbine automation system by upgrading it with notification signals if harsh weather conditions are detected in the prognostic horizon [66].

The high-altitude wind velocity data employed in this study was acquired in the wind-tunnel experiments performed at the Technical University of Munich, Germany, by simulating an atmospheric boundary layer at the simulation length scale factor $\lambda = 395$, calculated as suggested by [67]. The flow velocity was measured using a DANTEC 55P91 triple hot-wire probe and an AALAB AN 1003 anemometer system. Flow velocity was sampled at 1.25 kHz using a 12-bit digitizer Data Translation DT2821 during 150 s of the time records. In that way, in total 187,500 data samples were acquired at various points along the vertical axis above the turntable. A detailed presentation of the wind-tunnel measurement is available in [68], whereas an example of the wind velocity fluctuations at an altitude of 414 m (scaled-up to full-scale) is shown in Figure 5. Like a purse seiner, this wind velocity time record was employed using the MLMC program.

The acquired data (rounded off to the nearest integer) was considered in the case of three learning periods (50000 cycles, 100000 cycles, and 187500 cycles) and two prognostic horizons (100 and 1000 cycles) while calculating the associated probability distributions using the AS and MSM procedures. In the MSM case, only the first eigenvalue and the first eigenvector were considered in Eq. (10). The results obtained are presented in Table 2. In total, nine states were identified for the shortest learning period, while an additional wind velocity state of 10 m/s was detected in the remaining two cases. Similarly to the purse seiner case, all probability distributions obtained by the AS and MSM approaches exhibit very good agreement, with only negligible discrepancies observed for the shorter prognostic horizon (PH = 100 cycles), which may be attributed to transient effects. A very good agreement is evident between the expected and average wind velocities. Furthermore, the corresponding standard deviations closely match the statistical values, indicating that the proposed probabilistic framework can accurately assess both the mean behavior and the variability of the wind velocity process across all learning periods.

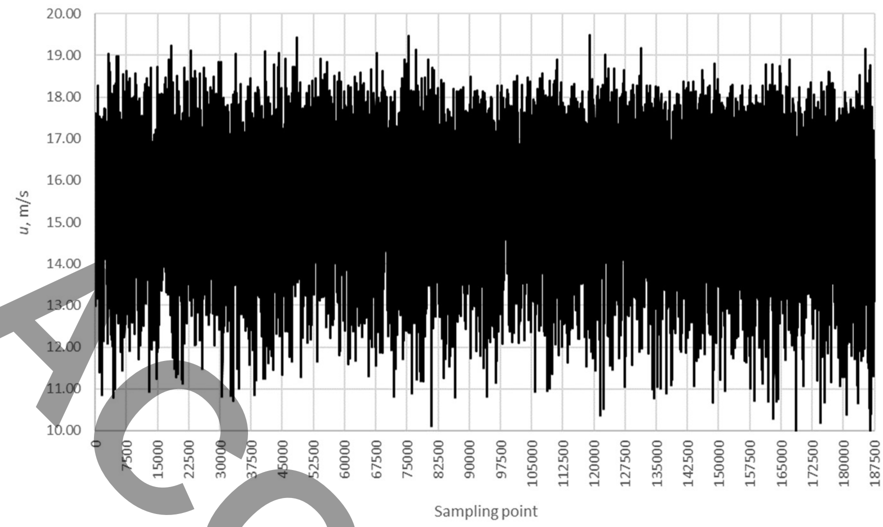

Figure 5. An example of the wind speed fluctuations at an altitude of 414 m

Table 2. Probability distributions and the expected high-altitude wind flow velocity determined for three learning periods (LP) and two prognostic horizons (PH)

	LP – 50000 cycles				LP – 100000 cycles				LP – 187500 cycles			
	PH=100 cycles (0.8 s)		PH=1000 cycles (8 s)		PH=100 cycles (0.8 s)		PH=1000 cycles (8 s)		PH=100 cycles (0.8 s)		PH=1000 cycles (8 s)	
Wind velocity, m/s	AS	MSM	AS	MSM	AS	MSM	AS	MSM	AS	MSM	AS	MSM
10	/	/	/	/	0.000	0.000	0.000	0.000	0.000	0.000	0.000	0.000
11	0.145	0.145	0.145	0.145	0.148	0.147	0.147	0.147	0.151	0.151	0.151	0.151
12	0.054	0.054	0.054	0.054	0.054	0.054	0.054	0.054	0.057	0.057	0.057	0.057
13	0.260	0.260	0.260	0.260	0.258	0.258	0.258	0.258	0.261	0.260	0.260	0.260
14	0.291	0.292	0.292	0.292	0.298	0.298	0.298	0.298	0.294	0.294	0.294	0.294
15	0.188	0.188	0.188	0.188	0.189	0.189	0.189	0.189	0.184	0.184	0.184	0.184
16	0.045	0.045	0.045	0.045	0.040	0.040	0.040	0.040	0.036	0.036	0.036	0.036
17	0.013	0.013	0.013	0.013	0.011	0.011	0.011	0.011	0.013	0.013	0.013	0.013
18	0.002	0.002	0.002	0.002	0.002	0.002	0.002	0.002	0.002	0.002	0.002	0.002
19	0.002	0.002	0.002	0.002	0.001	0.001	0.001	0.001	0.001	0.001	0.001	0.001
Expected wind velocity, u_E, and (standard deviation), m/s	15.507 (1.489)	15.508 (1.491)	15.508 (1.491)	15.508 (1.491)	15.503 (1.485)	15.504 (1.481)	15.504 (1.481)	15.504 (1.481)	15.460 (1.514)	15.461 (1.510)	15.461 (1.510)	15.461 (1.510)
Statistically average wind velocity, $\overline{u}$, and (standard deviation), m/s	15.508 (1.257)				15.504 (1.257)				15.461 (1.257)			
Absolute difference, $u_E - \overline{u}$, m/s	0.001	0	0	0	0.001	0	0	0	0.001	0	0	0

The LP–50000 case was further employed to evaluate wind velocity fluctuations over a prognostic horizon of 1000 cycles. For this purpose, the identified transition matrix was combined with a random number generator to simulate stochastic-state transitions. The prediction was initialized from a wind velocity of 15 m/s, corresponding to the 50000th measurement cycle. The resulting out-of-sample simulation uses the transition probabilities identified during the learning period to simulate the wind velocity trajectory beyond the training interval. The predicted trajectory is compared with the corresponding wind-tunnel measurements in Figure 6. It should be emphasized that the presented trajectory represents only one realization of the stochastic process, while numerous alternative trajectories can be cretaed from the same transition probability matrix.

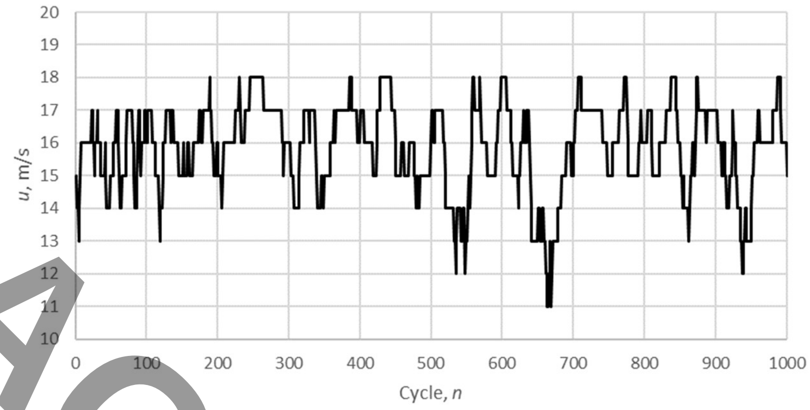

a)

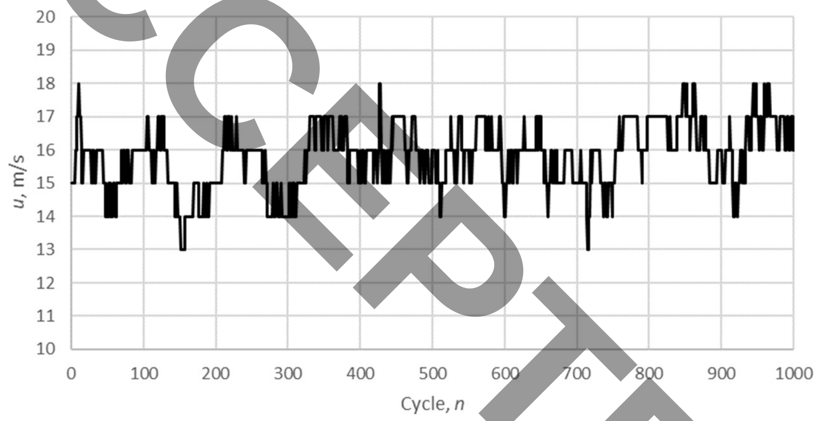

b)

Figure 6. a) The projected trajectory of the wind velocity fluctuations in comparison with b) wind-tunnel data, LP – 50000 cycles, PH – 1000 cycles

To evaluate the effect of the state discretization on the proposed framework, an additional analysis was performed using a finer state-space representation. In the previous example, the wind velocity was rounded to the nearest integer, yielding a total of ten system states. In contrast, the same dataset was discretized by rounding the wind velocity to the nearest tenth, yielding 93 states during the analyzed signal. This nearly tenfold increase in the number of states provides an effective sensitivity analysis of the proposed methodology with respect to the selected discretization level. The corresponding results obtained using the AS and MSM approaches are shown in Table 3. For brevity, only the expected average wind velocities are reported. It can be observed that the predicted wind velocities remain in very good agreement with the average values despite the substantially finer discretization. In particular, the MSM approach exhibits practically identical results for all analyzed prediction horizons, with absolute differences not exceeding 0.001 m/s. These results indicate that the proposed framework is largely insensitive to moderate changes in the discretization level, demonstrating that the predictive performance is governed primarily by the underlying stochastic process rather than by the choice of the state resolution.

Increasing the number of states inevitably leads to higher CPU time and memory requirements, particularly for the AS procedure, because of the increased size of the transition probability matrix. In practical engineering applications, the number of possible states may become considerably larger, making the direct AS approach computationally demanding or even impractical. In contrast, the MSM procedure remains highly resilient to the increase in problem size, since in most applications only the dominant eigenvector associated with the unit eigenvalue is required for evaluating the stationary behavior. Consequently, the proposed MSM-based framework preserves both computational efficiency and predictive accuracy even when a substantially finer discretization of the system state is adopted.

Table 3. The expected high-altitude wind velocity for three learning periods (LP) and two prognostic horizons (PH)

	LP – 50000 cycles				LP – 100000 cycles				LP – 187500 cycles			
	PH=100 cycles (0.8 s)		PH=1000 cycles (8 s)		PH=100 cycles (0.8 s)		PH=1000 cycles (8 s)		PH=100 cycles (0.8 s)		PH=1000 cycles (8 s)	
	AS	MSM	AS	MSM	AS	MSM	AS	MSM	AS	MSM	AS	MSM
Expected wind velocity, u_E, m/s	15.448	15.510	15.510	15.510	15.448	15.505	15.505	15.505	15.402	15.461	15.461	15.461
Average wind velocity, $\bar{u}$, m/s	15.508				15.504				15.461			
Absolute difference, $u_E - \bar{u}$, m/s	0.060	-0.002	-0.002	-0.001	0.056	-0.001	-0.001	-0.001	0.059	0	0	0

4 Discussion

Two modeling approaches, the analytical solution (AS) and the modal superposition method (MSM), were developed and applied in two test cases, i.e., purse seiner and high-altitude wind. The Mean Absolute Error (MAE) analysis confirms that there is a high level of consistency across both datasets, though the sailing speed of the purse seiner exhibits slightly more variance than the wind velocity. For the shortest time history, minor discrepancies of the sailing speed are observed, leading to a maximum MAE of 0.00424 km/h , and a consistent MAE of 0.0001 m/s for the wind velocity. As the time record length increases, these minor deviations are not present any more in all the test cases.

The reliability of the obtained data is important as it contains all the information employed to create the transition matrix in terms of system states, problem scale, and transition probabilities. Hence, both internal and external factors affecting the data acquisition process must be carefully considered. In the first case, internal uncertainties originate from measurement imperfections and characteristic sensor noise, which were reduced by applying the Kalman filter implemented in the MAPON and Data Translation DT2821 software. Moreover, the measurement system incorporates built-in protection mechanisms against irregular conditions, magnetic interference, and unauthorized manipulation, thereby enhancing the reliability and integrity of the obtained results prior to their use in the proposed framework. In the second case, external disturbances may be associated with variations in the operating profile of the monitored object, including environmental conditions and human control. While such effects are present in the case of the purse seiner, they may be considered negligible for the high-altitude wind-velocity fluctuations. A slight increase in the expected average sailing speed for longer learning periods may be attributed to changes in the operating profile of the ship due to market demands and the fish school dynamics.

The issue of CPU requirements is an important aspect, especially if agile and real-time decision-making is required. In such cases, the evaluation time must be significantly shorter than the sampling cycle. However, this may become challenging for the AS approach since it is based on repeated matrix multiplication, Eq. (5), with a computational complexity of $O(nd^3)$, where d is the state-space dimension and n is the prognostic horizon. Furthermore, the transition matrix requires $O(d^2)$ memory storage. In contrast, the MSM determines only the dominant eigenpair by employing the power method, yielding a computational complexity of approximately $O(kd^2)$, where k is the number of iterations required for convergence, while the memory requirement is reduced to $O(d)$ when only the dominant eigenvector is retained for the stationary solution. Therefore, the computational advantage of the MSM becomes increasingly significant as the problem scale grows.

This effect is illustrated by the wind velocity example, where increasing the discretization from integer values to tenths enlarges the state space from 10 to 93 states. Consequently, the transition matrix size increases from 10 × 10 (100 elements) to 93 × 93 (8649 elements), corresponding to an approximately 86-fold increase in the number of matrix elements and memory requirements of the AS approach. Nevertheless, a detailed discretization did not provide any significant improvement in the expected wind velocity, as demonstrated by the good agreement between the results presented in Tables 2 and 3. On the other hand, the results in Tables 1–3 show that both the AS and MSM procedures yield practically identical stationary probability distributions regardless of the prognostic horizon, indicating that the considered Markov chains operate in the steady-state domain. Therefore, for the MSM, it is sufficient to retain only the dominant eigenvalue and the associated eigenvector, whereas additional modes need to be considered only when transient effects are of interest [59].

Finally, some may argue that the application of stochastic processes is unnecessary in the considered examples, particularly because the expected average values exhibit very good agreement. Nevertheless, these statistical values were employed solely to validate the proposed modeling approaches. The principal advantage of stochastic processes lies in their ability to explicitly represent the inherent uncertainty of complex systems, thereby enabling predictive analysis and risk-informed decision-making. Such information may be employed to evaluate quantities including the first-passage time, expected return time, occupancy times, cost and gain horizons, bottleneck states, and the probabilistic trends of engineering systems [69]–[72]. It should be noted that the proposed framework is based on a first-order nonhomogeneous Markov chain, implying that future system evolution depends only on the current state. While this assumption is appropriate for many engineering systems exhibiting short-term stochastic dynamics, processes characterized by pronounced long-term temporal dependencies or partially observable states may require higher-order or Hidden Markov Models, representing a promising direction for future work.

Although the proposed framework has been assessed based on engineering applications, its underlying methodology is not limited to engineering systems. The developed nonhomogeneous Markov chain model may also be applied to stochastic biological processes characterized by sequential observations and continuously evolving state transitions, such as real-time electrocardiogram (ECG) monitoring, physiological signal analysis, or epidemic spread modeling. In such applications, the ability to continuously update predictions while maintaining low computational requirements and model interpretability may provide an attractive alternative for real-time decision support [73].

5 Conclusions

AI and ML are emerging technologies that enhance work productivity and performance, especially in cases where large bodies of data surpass human perception. Their intensive development and application in various fields of science and technology prove that they are the basis for the development of society and economy. This is particularly the case in real-time engineering. However, there are some wide-ranging challenges regarding the engineering applications of AI and ML, including modeling approaches, computational requirements, data storage, accuracy, and interpretability of the results.

This study contributes to these points by introducing a new concept of nonhomogeneous Markov chains based on the nonhomogeneous definition of the transition matrix and assessment of the associated state probability distributions by employing a rigorous analytical solution and the modal superposition method. Both methods were successfully employed in two cases representing a purse seiner and a high-altitude wind. Special attention was given to CPU requirements and the system space-scale issues with the new evaluation methodology integrated into an in-house MCML program. It was proven that the reduction of complex problems through the modal superposition method enables reliable and rational evaluation of the probability distributions even in the case when only the first eigenvalue and eigenvector are considered. This in turn significantly reduces computational demand while maintaining the accuracy of the results.

The proposed approach is not limited to the applications presented in the present study and may be extended to a broad range of engineering problems. Possible applications include the formal identification of bottleneck states and the design and optimization of systems based on the stochastic properties of variables, constraints, and objective functions. Future work should consider the extension of the MCML methodology to continuous-state Markov chains and systems involving functionally dependent variables. Such developments will facilitate the integration of nonhomogeneous Markov chains into AI and machine learning frameworks as efficient, robust, and interpretable probabilistic algorithms. Furthermore, the assumption of a first-order nonhomogeneous Markov chain should be revisited to assess whether higher-order or more complex state-transition models can further improve predictive accuracy. Another promising direction involves the development of hybrid Machine Learning models that combine the probabilistic interpretability and computational efficiency of nonhomogeneous Markov chains with data-driven techniques such as neural networks or reinforcement learning, thereby combining the complementary strengths of both approaches in complex engineering applications.

Acknowledgment

This work was supported by the Croatian Science Foundation under the project number HRZZ-IP-2022-10-9434. This paper has been funded by the European Union (NextGenerationEU) under the National Recovery and Resilience Plan 2021–2026 (NRRP), through the UNIZAG FSB institutional projects “Structural aerodynamics” and “Advanced methods for ship maintenance management-NEURON-B” approved by the Ministry of Science, Education and Youth of the Republic of Croatia (component C3.2, source 581).

References

[1] BJ. Copeland, “artificial intelligence,” Encyclopedia Britannica. https://www.britannica.com/technology/artificial-intelligence [Accessed: 15 March 2024].

[2] European Commission, *Communication from the Commission to the European Parliament*, the European Economic and Social Committee, and the Committee of Regions: *Fostering a European Approach to Artificial Intelligence*, Brussels, 2021

[3] European Commission, *Proposal for a Regulation of the European Parliament and of the Council laying down harmonised rules on artificial intelligence (Artificial Intelligence Act) and amending certain Union legislative acts*, Brussels, Belgium, 2021

[4] R. I. Mukhamediev, Y. Popova, Y. Kuchin, E. Zaitseva, A. Kalimoldayev, A. Symagulov, V. Levashenko, F. Abdolina, V. Gopejenko, K. Yakunin, E. Muhamedijeva, and M. Yelis, “Review of artificial intelligence and machine learning technologies: Classification, restrictions, opportunities and challenges,” *Mathematics*, vol. 10, no. 15, 2022, doi: 10.3390/math10152552.

[5] C. S. Song and J.-H. Nam, “Machine learning-based optimal value calculation for welding variables in AR training,” *Int. J. Nav. Archit. Ocean Eng.*, vol. 17, 2025, doi: 10.1016/j.ijnaoe.2025.100652.

[6] R. H. Jhaveri, A. Revathi, K. Ramana, R. Raut, and R. K. Dhanaraj, “A review on machine learning strategies for real-world engineering applications,” *Hindawi Adv. Mech. Eng.*, vol. 2022, Art. no. 1833507, 2022, doi: 10.1155/2022/1833507

[7] H. Pishro-Nik, *Practical Uncertainty*. Kappa Research, USA, 2023.

[8] Y. F. Guo, J. K. Liu, Y. S. Ma, and R. Ahmad, "Deep learning-based topology optimization for multi-axis machining," *Applied Mathematical Modelling*, vol. 138, 2024, doi: 10.1016/j.apm.2024.115738.

[9] J. Lee, S. M. Bateni, C. Jun, E. Heggy, M. Jamei, D. Kim, H. R. Ghafouri, and J. L. Deenik, "Hybrid machine learning system based on multivariate data decomposition and feature selection for improved multitemporal evapotranspiration forecasting," *Engineering Applications of Artificial Intelligence*, vol. 135, 2024, doi: 10.1016/j.engappai.2024.108744.

[10] S. Nam, Y. Cho, and J. H. Woo, "Simulation-based deep reinforcement learning for multi-objective identical parallel machine scheduling problem," *International Journal of Naval Architecture and Ocean Engineering*, vol. 16, 2024, doi: 10.1016/j.ijnaoe.2024.100629.

[11] E. Y. Son, D. Jeong, and M. J. Oh, "Corrosion area detection and depth prediction using machine learning," *International Journal of Naval Architecture and Ocean Engineering*, vol. 16, 2024, doi: 10.1016/j.ijnaoe.2024.100617.

[12] Y. Zhao, Y. Huang, Z. Wang, and X. Liu, "Carbon futures price forecasting based on feature selection," *Engineering Applications of Artificial Intelligence*, vol. 135, 2024, doi: 10.1016/j.engappai.2024.108646.

[13] F. Schweitzer, L. Habel, O. J. Canaviri Vilca, T. Kulzer, and S. Wenzel, "Advancing production planning in the automotive industry: machine learning-enhanced simulation optimization using metamodels," *Journal of Simulation*, 1–17, 2025, doi: 10.1080/17477778.2025.2532661.

[14] Q. Zhao, J. Blake, M. Taghavi, and P. Vanberkel, "Combining simulation and machine learning in

healthcare: a literature review," *Journal of Simulation*, 1–15, 2025, doi: 10.1080/17477778.2025.2549092.

[15] I. Ozsari, "Predicting main engine power and emissions for container, cargo, and tanker ships with artificial neural network analysis," *Brodogradnja*, vol. 74, pp. 77–94, 2023, doi: 10.21278/brod74204.

[16] R. Qin, L. Wang, X. Du, J. Chen, X. Chen, and B. Yan, "Adversarial robust decision-making under uncertainty learning and dynamic ensemble selection," *Engineering Applications of Artificial Intelligence*, vol. 135, 2024, doi: 10.1016/j.engappai.2024.108653.

[17] K. Poyyathappan, S. Dinesh, A. Ganeshkumar, and M. Arul, "Harnessing machine learning for wear prediction in sustainable fibre-reinforced hybrid composites," *Transactions of FAMENA*, vol. 49, pp. 31–44, 2025, doi: 10.21278/TOF.492069324.

[18] J. Vijayanand and S. R. Vaddi, "An artificial neural network model supported with hybrid multi-criteria decision-making approaches to rank lean tools for a foundry industry," *Transactions of FAMENA*, vol. 48, pp. 245–268, 2024, doi: 10.7166/35-1-2906.

[19] M. B. Saad, Q. Al-Tashi, L. Hong, et al., "Machine-learning driven strategies for adapting immunotherapy in metastatic NSCLC," *Nat. Commun.*, vol. 16, 6828, 2025, doi: 10.1038/s41467-025-61823-w.

[20] G. Kostopoulos, G. Davrazos, and S. Kotsiantis, "Explainable Artificial Intelligence-Based Decision Support Systems: A Recent Review." Electronics, 13(14), 2024, 2842, doi: 10.3390/electronics13142842.

[21] S. Moosavi, M. Farajzadeh-Zanjani, R. Razavi-Far, V. Palade, and M. Saif, "Explainable AI in Manufacturing and Industrial Cyber–Physical Systems: A Survey," Electronics, 13(17), 2024, 3497, doi: 10.3390/electronics13173497.

[22] A. Elhanashi, S. Essahraui, P. Dini, D. Paolini, Q. Zheng, S. Saponara, "Generative AI and the Foundation Model Era: A Comprehensive Review," Big Data Cogn. Comput. 2026, 10, 94 doi: 10.3390/bdcc10030094.

[23] K. S. Awaisi, Q. Ye, and S. Sampalli, "A Survey of Industrial AIoT: Opportunities, Challenges, and Directions," IEEE Access, vol. 12, 2024, pp. 103596–103636, doi: 10.1109/ACCESS.2024.3426279.

[24] Ł. Korycki and B. Krawczyk, "Class-Incremental Learning: A Survey," Pattern Recognition, vol. 155, 2024, Art. no. 110702, doi: 10.1016/j.patcog.2024.110702.

[25] Y. LeCun, B. Kerbl, T. Darrell, A. Efros, R. Fergus, J. Malik, et al., "Machine Learning for Computer Vision," Proceedings of the IEEE, vol. 113, no. 1, pp. 1–31, 2025.

[26] N. Hadžić, "Analytical solution of the serial Bernoulli production line steady-state performance and its application in the shipbuilding process," *International Journal of Production Research*, vol. 57, pp. 1052–1065, 2019, doi: 10.1080/00207543.2018.1500042.

[27] N. Hadžić, V. Ložar, and F. Abdulaj, "A finite state method in the performance evaluation of the Bernoulli serial production lines," *Applied Sciences*, vol. 10, pp. 1–23, 2020, doi: 10.3390/app10186602.

[28] L. Wang, X. Zhang, H. Su, and J. Zhu, "A Comprehensive Survey of Continual Learning: Theory, Method and Application," IEEE Transactions on Pattern Analysis and Machine Intelligence, vol. 46, no. 8, pp. 5362–5383, 2024, doi: 10.1109/TPAMI.2024.3367329.

[29] J. Lian, K. Choi, B. Veeramani, A. Hu, S. Murli, L. Freeman, E. Bowen, and X. Deng, "Continual Learning and Its Industrial Applications: A Selective Review," WIREs Data Mining and Knowledge Discovery, vol. 14, no. 6, 2024, Art. no. e1558, doi: 10.1002/widm.1558.

[30] H. Tyralis and G. Papacharalampous, "A Review of Predictive Uncertainty Estimation with Machine Learning," Artificial Intelligence Review, vol. 57, 2024, Art. no. 94, doi: 10.1007/s10462-023-10698-8.

[31] F. Mauro and R. Nabergoj, "Probabilistic evaluation of dynamic positioning operability with a Quasi-Monte Carlo approach," *Brodogradnja*, vol. 75, 75105, 2024, doi: 10.21278/brod75105.

[32] J. Gao and Y. Zhang, "Ship collision avoidance decision-making research in coastal waters considering uncertainty of target ships," *Brodogradnja*, vol. 75, 75203, 2024, doi: 10.21278/brod75203.

[33] J. C. J. Prince and K. Lingadurai, "The hybrid approach of a machine learning algorithm for addressing the permutation flow-shop scheduling problem," *Transactions of FAMENA*, vol. 49, pp. 77–88, 2025, doi: 10.21278/TOF.492062623.

[34] K. P. Murphy, Probabilistic Machine Learning: Advanced Topics. Cambridge, MA, USA: MIT Press, 2023.

[35] S. Z. Yu, "Hidden semi-Markov models," *Artificial Intelligence*, vol. 174, pp. 215–243, 2010, doi: 10.1016/j.artint.2009.11.011.

[36] V. Gogate and R. Dechter, "SampleSearch: Importance sampling in presence of determinism," *Artificial Intelligence*, vol. 175, pp. 694–729, 2011, doi: 10.1016/j.artint.2010.10.009.

[37] F. Pirri, 'The well-designed logical robot: Learning and experience from observations to the Situation Calculus', *Artificial Intelligence*, vol. 175, no. 1, pp. 378–415, Jan. 2011, doi: 10.1016/j.artint.2010.04.016.

[38] T. Tran, D. Phung, H. Bui, and S. Venkatesh, "Hierarchical semi-Markov conditional random fields for deep recursive sequential data," *Artificial Intelligence*, vol. 246, pp. 53–85, 2017, doi: 10.1016/j.artint.2017.02.003.

[39] S. Y. Chong, P. Tino, and J. He, "Coevolutionary systems and PageRank," *Artificial Intelligence*, vol. 277, 2019, doi: 10.1016/j.artint.2019.103164.

[40] M. Schuurmans, A. Katriniok, C. Meissen, H. E. Tseng, and P. Patrinos, "Safe, learning-based MPC for highway driving under lane-change uncertainty: A distributionally robust approach," *Artificial Intelligence*, vol. 320, 2022, doi: 10.1016/j.artint.2023.103920.

[41] S. Shao, S. McAleer, R. Yan, and P. Baldi, "Artificial Intelligence for Digital Twins and Predictive Maintenance in Industry 4.0: A Review," Engineering Applications of Artificial Intelligence, vol. 132, 2024, Art. no. 108077, doi: 10.1016/j.engappai.2024.108077.

[42] X. Yang, Y. Liu, H. Zhang, and J. Lee, "Markov Models for Prognostics and Health Management: A Review of Recent Advances," Reliability Engineering & System Safety, vol. 247, 2024, Art. no. 110132, doi: 10.1016/j.ress.2024.110132.

[43] G. Padula, M. Girfoglio, and G. Rozza, "A Brief Review of Reduced Order Models Using Intrusive and Non-Intrusive Techniques," Proceedings in Applied Mathematics and Mechanics, vol. 24, 2024, Art. no. e202400210, doi: 10.1002/pamm.202400210.

[44] B. Kramer, B. Peherstorfer, and K. E. Willcox, "Learning Nonlinear Reduced Models from Data with Operator Inference," Annual Review of Fluid Mechanics, vol. 56, pp. 521–548, 2024, doi: 10.1146/annurev-fluid-121021-025220.

[45] Y. Shi, P. Wei, K. Feng, D.-C. Feng, and M. Beer, "A Survey on Machine Learning Approaches for Uncertainty Quantification of Engineering Systems," Machine Learning for Computational Science and Engineering, vol. 1, Art. no. 11, 2025.

[46] G. Wolfer and A. Kontrokovich, "Learning and identity testing of Markov chains," in *Artificial Intelligence*, S. G. Krantz, A. S. R. S. Rao, and C. R. Rao, Eds. London: Elsevier, 2023.

[47] A. Adikari, G. Gamage, D. de Silva, N. Mills, S. M. J. Wong, and D. Alahakoon, "A self-structuring artificial intelligence framework for deep emotions modeling and analysis on the social web," *Future Generation Computer Systems*, vol. 116, pp. 302–315, 2021, doi: 10.1016/j.future.2020.10.028.

[48] F. Deufel, M. Giessler, and F. Gauterin, "A generic prediction approach for optimal control of electrified vehicles using artificial intelligence," *Vehicles*, vol. 4, pp. 182–198, 2022, doi: 10.3390/vehicles4010012

[49] C. Fan, S. H. Law, S. Ibrahim, and N. A. M. Naseem, "Research on the correlation between information and communication technology development and consumer spending based on artificial intelligence and time series econometric model," *Journal of Electrical and Computer Engineering*, vol. 2022, doi: 10.1155/2022/1645232

[50] Y. X. Wei, H. Bin Hashim, S. H. Lai, K. L. Chong, Y. F. Huang, A. N. Ahmed, M. Sherif, and A. El-Shafie, "Comparative analysis of artificial intelligence methods for streamflow forecasting," *IEEE Access*, vol. 12, pp. 10865–10885, 2024, doi: 10.1109/ACCESS.2024.3351754

[51] K. H. Bae and H. J. Ko, "Installation planning for an offshore wind farm: A hybrid modelling framework of integrating simulation and optimisation with a Markov chain," *Journal of Simulation*, vol. 19, no. 2, pp. 197–214, 2023, doi: 10.1080/17477778.2022.2163933

[52] M. Lei, L. Shiyan, J. Chuanwen, L. Hingling, and Z. Yan, "A review on the forecasting of wind speed and generated power," *Renewable and Sustainable Energy Reviews*, vol. 13, pp. 915–920, 2009, doi: 10.1016/j.rser.2008.02.002

[53] H. Tian, X. F. Wang, M. A. Mohammad, G. Y. Gou, F. Wu, Y. Yang, and T. L. Ren, "A hardware Markov chain algorithm realized in a single device for machine learning," *Nature Communications*, vol. 9, no. 1, p. 4305, Oct. 2018, doi: 10.1038/s41467-018-06644-w

[54] M. Ali, R. C. Deo, N. J. Downs, and T. Maraseni, "Multi-stage hybridized online sequential extreme learning machine integrated with Markov Chain Monte Carlo copula-Bat algorithm for rainfall forecasting," *Atmos. Res.*, vol. 213, pp. 450–464, 2018, doi: 10.1016/j.atmosres.2018.07.005.

[55] T. Mizutani, T. Kobayashi, and K. Teramoto, "Infrastructure Deterioration Modeling with an Inhomogeneous Continuous-Time Markov Chain: A Latent State Approach with Analytic Transition Probabilities," Computer-Aided Civil and Infrastructure Engineering, vol. 38, no. 13, pp. 1730–1748, 2023, doi: 10.1111/mice.12976.

[56] U. Khadam, P. Davidsson, and R. Spalazzese, "Exploring the Role of Artificial Intelligence in Internet of Things Systems: A Systematic Mapping Study," Sensors, vol. 24, no. 20, 2024, Art. no. 6511, doi: 10.3390/s24206511.

[57] E. Villar, I. Martín Toral, I. Calvo, O. Barambones, and P. Fernández-Bustamante, "Architectures for Industrial AIoT Applications," Sensors, vol. 24, no. 15, 2024, Art. no. 4929, doi: 10.3390/s24154929.

[58] V. G. Kulkarni, *Introduction to Modeling and Analysis of Stochastic Systems*, London: Springer, 2011.

[59] N. Hadžić, V. Ložar, T. Opetuk, and R. Keser, "Transient response of homogenous and nonhomogenous Bernoulli production lines," *Mathematics*, vol. 11, 2023, doi: 10.3390/math11244945.

[60] R. Gallager, *Discrete Stochastic Processes*, Cambridge, MA, USA: MIT Press, 2022.

[61] E. Kreyszig, *Advanced Engineering Mathematics*, New York, USA: Wiley, 2011.

[62] J. A. Nicholson, *Introduction to Programming Using Fortran 95*, 2011. [Online]. Available: https://www.fortrantutorial.com/

[63] M. Koričan, N. Vladimir, and A. Fan, "Investigation of the energy efficiency of fishing vessels: Case study of the fishing fleet in the Adriatic Sea," *Ocean Eng.*, vol. 286, 2023, doi: 10.1016/j.oceaneng.2023.115734.

[64] M. Koričan, N. Vladimir, T. Haramina, V. Slapničar, and N. Alujević, "Investigation of energy efficiency of fishing vessels in the Adriatic Sea by fuel consumption measurements and catch analysis: Design and operation of data collection system," in *2022 IEEE Canadian Conf. Electr. Comput. Eng. (CCECE)*, Halifax, NS, Canada, 2022, pp. 348–353, doi: 10.1109/CCECE49351.2022.9918264.

[65] MAPON, "Fleet Management & Asset Tracking Platform," 2024. [Online]. Available: https://www.mapon.com/en

[66] H. Kozmar, N. Hadžić, I. Ćatipović, and S. Rudan, "Wind load assessment in marine and offshore engineering standards," *Ocean Eng.*, vol. 252, 2022, doi: 10.1016/j.oceaneng.2022.110872.

[67] N. J. Cook, "Determination of the model scale factor in wind-tunnel simulations of the adiabatic atmospheric boundary layer," *J. Wind Eng. Ind. Aerodyn.*, vol. 2, pp. 311–321, 1978, doi: 10.1016/0167-6105(78)90016-8.

[68] H. Kozmar, "Physical modeling of complex airflows developing above rural terrains," *Environ. Fluid Mech.*, vol. 12, pp. 209–225, 2012, doi: 10.1007/s10652-011-9224-1.

[69] N. Hadžić, V. Ložar, T. Opetuk, and J. Andrić, "A finite state method in improvement and design of lean Bernoulli serial production lines," *Comput. Ind. Eng.*, vol. 158, p. 107449, 2021, doi: 10.1016/j.cie.2021.107449.

[70] N. Hadžić, V. Ložar, T. Opetuk, and J. Andrić, "The Bernoulli splitting line: Analytical and semi-analytical evaluation of the steady-state performance," *Int. J. Prod. Res.*, vol. 1, p. 47, 2021, doi: 10.1080/00207543.2021.1974115.

[71] N. Hadžić, V. Ložar, T. Opetuk, and Z. Kunkera, "The Bernoulli assembly line: The analytical and semi-analytical evaluation of steady-state performance," *Appl. Sci.*, vol. 12, pp. 1–30, 2022, doi: 10.3390/app122312447.

[72] V. Ložar, N. Hadžić, T. Opetuk, and V. Slapničar, "Accuracy of semi-analytical and numerical approaches in the evaluation of serial Bernoulli production lines," *Mathematics*, vol. 9, p. 1461, 2021, doi: 10.3390/math9131461.

[73] A. A. Alaa and M. van der Schaar, "Attentive State-Space Modeling of Disease Progression." Advances in Neural Information Processing Systems, 2017.